Strapdown Attitude Computation: Functional Iterative Integration versus Taylor Series Expansion

Yuanxin Wu[1]
Shanghai Jiao Tong University, Shanghai, 200240, China

and
Yury A. Litmanovich[2]
Central Scientific and Research Institute "Elektropribor", Saint Petersburg, 197046, Russia

There are two basic approaches to strapdown attitude computation, namely, the traditional Taylor series expansion approach and the Picard iterative method. The latter was recently implemented in a recursive form basing on the Chebyshev polynomial approximation and resulted in the so-called functional iterative integration approach. Up to now a detailed comparison of these two approaches with arbitrary number of gyroscope samples has been lacking for the reason that the first one is based on the simplified rotation vector equation while the second one uses the exact form. In this paper, the mainstream algorithms are considerably extended by the Taylor series expansion approach using the exact differential equation and recursive calculation of high-order derivatives, and the functional iterative integration approach is re-implemented on the normal polynomial. This paper applies the two approaches to solve the strapdown attitude problem, using the attitude parameter of quaternion as a demonstration. Numerical results under the classical coning motion are reported to assess all derived attitude algorithms. It is revealed that in the low and middle relative conic frequency range all algorithms have the same order of accuracy, but in the range of high relative frequency the algorithm by the functional iterative integration approach performs the best in both accuracy and robustness if the Chebyshev polynomials and a larger number of gyroscope samples are to be used. The main conclusion applies to other attitude parameters as well.

I. Introduction

ATTITUDE information is vitally important for moving objects in many areas including unmanned vehicle navigation and control, virtual/augmented reality, satellite communication, robotics, and computer vision [1]. Integrating gyroscope-measured angular velocity information is an essential and self-contained way to acquire the attitude, rotation or orientation [2-5]. Several orientation parameters have been used for attitude computation, including but not limited to the Euler angle, the rotation vector, the direction

[1] Professor, School of Electronic Information and Electrical Engineering.
[2] Head of Department.

cosine matrix and the quaternion. Attitude computation is in essence to numerically solve the ordinary differential equations of these attitude parameters. In the early stage of strapdown inertial navigation systems, Savage [6] tried the Picard-type iterative technique to integrate the direction cosine rate equation, and the NASA technical report [7] made the angular velocity polynomial approximation from a sequence of gyroscope outputs and then integrated the direction cosine matrix rate by the Runge-Kutta method. Shortly after in the 1970s, the modern-day strapdown attitude algorithm structure was established on the Taylor series expansion approach by Jordan and Bortz [8, 9], which, without exception, has relied on the approximate rotation vector for incremental attitude update [10-17]. The seminal paper by Miller [10] used a low-order Taylor series with low-order angular velocity approximation to solve the approximate rotation vector rate equation. Very recently, the Taylor series approach is employed to directly solve the direction cosine matrix rate equation [18], kind of a retrospective work into the early attempt [7]. The seminal Russian book in 1970s by Branets and Shmyglevsky [19] used the Taylor series approach to solve the rotation vector and the Picard-type successive approximation method to solve the attitude quaternion. The same approaches were applied by Panov to derive and analyze the multi-sample attitude algorithms which were summarized later in [20]. In parallel, a number of related fields mostly employ the quaternion to deal with attitude computation, e.g., robotics [21, 22], space applications [23] and computational mathematics [24-26], where the structure-preserving attribute of geometric integration is mostly concerned.

Another trend of intensive investigation in the strapdown attitude research was the ad-hoc algorithm optimization by means of special tuning of the algorithm coefficients to reduce the coning drift under the assumed motions such as the classical/generalized coning motion, the regular precession and the stochastic angular motion. It is based either on the comparison of expressions for rotation vector solution and gyroscope sample vector products under the coning [10-12, 17, 27-30] or on the general solution for rotation vector expressed via the angular rate polynomial coefficients and the relation between the former under the coning [10-12, 17, 27-29]. The cost one should pay is that the optimized algorithms rank below the corresponding original algorithms in accuracy in practically irregular angular motions, say maneuvers [16]. Needless to say it is desirable for algorithms to exhibit the same order of accuracy regardless of input attitude motions. These properties are hopefully acquired by the algorithms which use angular rate multiple integrals as input signals [31].

Special efforts were directed to derive the algorithms addressing the inherent gyroscope instrumental noise. Two alternative approaches were developed to reduce the pseudo-coning: one was aimed to introduce the smoothing properties to the algorithm by using the angular rate multiple integrals as input signals [31]; the other was reduced to the special tuning of the conventional algorithm coefficients taking into account the frequency shaping of the gyroscope signals when digital prefiltering is used to suppress the gyroscope noise [5, 32].

Although it is commonly believed that the modern-day attitude algorithm is good enough for most applications [13, 15, 33], the new dynamic applications and the future precision gyroscopes [34, 35] can demand more accurate attitude algorithms, in view of the practically limited gyroscope output rate and the fundamental approximation of modern-day algorithms. For instance, Ignagni [36] newly stresses the potentially significant accuracy loss of the mainstream attitude algorithm due to the neglected third

term (in contrast to the common belief above) and advises algorithmic enhancement for sustained highly dynamic motions, contrary to Savage's over-optimistic assertion that the modern-day algorithms have accuracy exceeding forecasted future requirements [33]. In principle, the recent advances in [18, 37-42] have shown that higher attitude accuracy can be achieved by dealing with better or exact rate forms of attitude parameters and using high-order numerical integration methods [43-45]. For instance, the impact of commonly-neglected third term in the rotation rate vector was evaluated in [29, 46] and it was partially incorporated in the algorithms to gain significant accuracy in dynamic applications [31, 38, 47]. The Rodrigues vector and the quaternion were used for attitude computation by way of functional iterative integration and Chebyshev polynomial approximation in [39-41]. The functional iterative integration approach combined with Chebyshev polynomial approximation was developed independently in the navigation community [39-41, 48-51], and lately found to closely resemble the so-called Picard-Chebyshev method that was dated back to as early as 1960s [52]. The Picard-type successive approximation is actually identical to the functional iterative integration approach applied to linear differential equation, as shown in [41].

It should be noted that the angular velocity polynomial approximation from a sequence of gyroscope outputs, which defines one part of the attitude computation error, is an integral part of both approaches [7, 10, 16, 29, 31, 43, 44], explicitly or implicitly. (Hereby in this paper we consider zero and single integral of angular velocity as gyroscope measurements because they are common in real systems, although multiple integrals could also be accounted for as done in [29, 31, 53]). The other part of the attitude computation error arises from solving the original differential equation by different methods.

This paper was motivated by a long fruitful discussion of the two authors about the actual accuracy superiority of the functional iterative approach over the traditional Taylor expansion approach. To make a reasonable comparison of two approaches, the mainstream algorithms have been considerably extended by the Taylor series expansion approach using the exact differential equation and recursive calculation of high-order derivatives, and the functional iterative integration approach was re-implemented on the normal polynomial. The computational aspect of the algorithm implementation is put aside as the recursive (cyclic) form of the algorithms under examination allow for using hardware realization, such as PLD (FPGA).

The paper exemplifies the comparison using the quaternion for brevity and we stress that the main conclusion obtained in this paper also applies to other attitude parameters [54]. The remainder of the paper is organized as follows: Section II briefly reviews two basic approaches to solve the ordinary differential equations, namely, the Taylor series expansion and the functional iterative integration. Section III discusses angular velocity approximation by the normal polynomial and the Chebyshev polynomial, and then Sections IV makes use of the two basic approaches to solve the kinematic equations of attitude quaternion. The reason that the functional iterative integration approach is re-implemented by the normal polynomial in addition to the Chebyshev polynomial in the original papers is that the mainstream algorithms actually used the normal polynomial in Taylor expansion. By so doing, the functional iterative integration approach is to be more sufficiently assessed against the Taylor expansion. Section V comprehensively assesses all derived algorithms under the classical coning motion by simulation. A summary is given in the last section of the paper.

II. General Approaches to Solve Ordinary Differential Equation

Without the loss of generality, consider an ordinary differential equation over a time interval $[0 \;\; t]$

$$\dot{\mathbf{y}} = \mathbf{f}(\mathbf{y}, t) \tag{1}$$

where $\mathbf{f}(\mathbf{y}, t)$ is an infinitely smooth function and the initial value of $\mathbf{y}$ is given by $\mathbf{y}(0)$.

The solution to (1) could be obtained by the Taylor series expanded at $t = 0$

$$\mathbf{y}(t) = \mathbf{y}(0) + \dot{\mathbf{y}}(0)t + \ddot{\mathbf{y}}(0)\frac{t^2}{2!} + \cdots = \sum_{j=0}^{\infty} \mathbf{y}^{(j)}(0)\frac{t^j}{j!} \tag{2}$$

in which $\mathbf{y}^{(j)}(0) = \mathbf{y}^{(j)}(t)\big|_{t=0}$, that is, the value of the j-th derivative at $t = 0$. The series is infinite and keeping terms up to the m-th order leads to a Taylor series approximation as follows [43]

$$\mathbf{y}(t) = \sum_{j=0}^{m} \mathbf{y}^{(j)}(0)\frac{t^j}{j!} + \mathbf{y}^{(m+1)}(\varsigma)\frac{t^{m+1}}{(m+1)!}, \quad \varsigma \in [0 \;\; t] \tag{3}$$

The second term on the right side characterizes the error of the m-th order Taylor series approximation. It is commonly conceived that the calculation of high-order derivatives involved is time-consuming and tedious, though conceptually straightforward [43]. In fact, the high-order derivatives share the common property that only their values at $t = 0$ are required and thus we need not know the analytic forms of the derivatives. The values of the high-order derivatives could be recursively computed by making use of the calculus rule of elementary functions [44, 55]. For example, assume $\mathbf{f}(\mathbf{y}, t) = \mathbf{y}(t)\mathbf{u}(t)$, then

$$\mathbf{y}^{(j)}(0) = \left(\mathbf{y}(t)\mathbf{u}(t)\right)^{(j-1)}\Big|_{t=0} = \left(\dot{\mathbf{y}}(t)\mathbf{u}(t) + \mathbf{y}(t)\dot{\mathbf{u}}(t)\right)^{(j-2)}\Big|_{t=0} = \ldots = \sum_{i=0}^{j-1}\binom{j-1}{i}\mathbf{y}^{(i)}(0)\mathbf{u}^{(j-1-i)}(0),$$

where $\binom{m}{k}$ denotes the number of combinations taking k elements from m elements. It means that high-order derivatives at some instant can be represented by low-order derivatives at the same instant, which provides an economical way to compute the Taylor series approximation [44, 55].

Furthermore, the solution to (1) could alternatively be obtained by the Picard iteration or a kind of functional iterative integration as [55]

$$\mathbf{y}_j(t) = \mathbf{y}(0) + \int_0^t \mathbf{f}(\mathbf{y}_{j-1}(t), t)\,dt, \quad j = 1, 2, \ldots \tag{4}$$

where the initial function over the integration interval could be set to $\mathbf{y}_0(t) = \mathbf{y}(0)$. It can be proved that the difference between the (m-1)-th and the m-th iterations [55]

$$\left\|\mathbf{y}_m(t) - \mathbf{y}_{m-1}(t)\right\| \le W L^{m-1}\frac{t^m}{m!} \tag{5}$$

if the function $\mathbf{f}$ is bounded by W, namely $W = \max_{\tau \in [0\, t]}\left\|\mathbf{f}(\mathbf{y}, \tau)\right\|$, and satisfies the Lipschitz continuity condition $\left\|\mathbf{f}(\mathbf{y}, t) - \mathbf{f}(\mathbf{z}, t)\right\| \le L\left\|\mathbf{y} - \mathbf{z}\right\|$. The right side of (5) is a term of the Taylor

series for e^{Lt} up to a scale. By the Weierstrass M-Test [56], the above sequence $\{\mathbf{y}_j\}_{j=0}^{\infty}$ converges uniformly to the true solution. The practical drawback of (4) is the repeated computation of integrals. It was surmounted in practice, for the first time to our best knowledge, by the Chebyshev polynomial approximation of the function $\mathbf{f}$ in [52]. Of course, the normal polynomial could alternatively be used.

It should be highlighted hereby that the Taylor series approximation in (3) is in itself of the normal polynomial, while the Picard iteration in (4) naturally accommodates any kind of polynomial.

III. Angular Velocity Polynomial Fitted from Gyroscope Measurements

The above two basic approaches in last section requires $\mathbf{f}(\mathbf{y},t)$ to be analytically known, but for the attitude computation under investigation, only the equally-spaced discrete gyroscope measurements are available. A common practice is to approximate the angular velocity by a polynomial fitted from the discrete gyroscope measurements [7, 10, 16, 29, 31, 43, 44]. The main content of this section has been presented in [39-41] and is repeated here for easy reference.

Assume discrete measurements (or called samples) of angular velocity $\boldsymbol{\omega}_k$ or angular increment $\Delta\boldsymbol{\theta}_k$ are available by a triad of gyroscopes at time instants $t_k = kT$ ($k = 1, 2, \ldots N$), where T denotes the sampling interval.

A. Normal Polynomial

The angular velocity can be approximated over the time interval $[0 \;\; t]$ by a normal polynomial as

$$\boldsymbol{\omega}(t) = \sum_{i=0}^{n} \mathbf{d}_i t^i, \;\; n \le N-1 \tag{6}$$

where the coefficient $\mathbf{d}_i$ is determined using the discrete angular velocity or angular increment measurements. The derivatives of the fitted angular velocity can be readily obtained as $\boldsymbol{\omega}^{(j)}(0) = j!\mathbf{d}_j$ for $j \le n$ and $\boldsymbol{\omega}^{(j)}(0) = 0$ otherwise.

For the case of angular velocity measurement, the coefficients $\mathbf{d}_i$ satisfy the equation

$$\begin{bmatrix} 1 & t_1 & \cdots & t_1^n \\ 1 & t_2 & \cdots & t_2^n \\ \vdots & \vdots & \vdots & \vdots \\ 1 & t_N & \cdots & t_N^n \end{bmatrix} \begin{bmatrix} \mathbf{d}_0^T \\ \mathbf{d}_1^T \\ \vdots \\ \mathbf{d}_n^T \end{bmatrix} = \begin{bmatrix} \boldsymbol{\omega}_1^T \\ \boldsymbol{\omega}_2^T \\ \vdots \\ \boldsymbol{\omega}_N^T \end{bmatrix} \tag{7}$$

And for the case of angular increment measurement instead, the coefficients satisfy

$$\begin{bmatrix} t_1 & \frac{t_1^2}{2} & \cdots & \frac{t_1^{n+1}}{n+1} \\ t_2-t_1 & \frac{t_2^2-t_1^2}{2} & \cdots & \frac{t_2^{n+1}-t_1^{n+1}}{n+1} \\ \vdots & \vdots & \vdots & \vdots \\ t_N-t_{N-1} & \frac{t_N^2-t_{N-1}^2}{2} & \cdots & \frac{t_N^{n+1}-t_{N-1}^{n+1}}{n+1} \end{bmatrix} \begin{bmatrix} \mathbf{d}_0^T \\ \mathbf{d}_1^T \\ \vdots \\ \mathbf{d}_n^T \end{bmatrix} = \begin{bmatrix} \Delta\boldsymbol{\theta}_1^T \\ \Delta\boldsymbol{\theta}_2^T \\ \vdots \\ \Delta\boldsymbol{\theta}_N^T \end{bmatrix} \tag{8}$$

B. Chebyshev Polynomial

The Chebyshev polynomial is a sequence of orthogonal polynomial bases and has better numerical stability than the normal polynomial [45]. The Chebyshev polynomial of the first kind is defined over the interval $[-1 \quad 1]$ by the recurrence relation as

$$F_0(x)=1, F_1(x)=x, F_{i+1}(x)=2xF_i(x)-F_{i-1}(x) \tag{9}$$

where $F_i(x)$ is the i^{th}-degree Chebyshev polynomial of the first kind. For any $j,k \geq 0$, the Chebyshev polynomial of first kind satisfies the equality [45]

$$F_j(\tau)F_k(\tau)=\frac{1}{2}\left(F_{j+k}(\tau)+F_{|j-k|}(\tau)\right) \tag{10}$$

In order to apply the Chebyshev polynomial, the actual time interval $[0 \quad t_N]$ is mapped onto $[-1 \quad 1]$ by letting $t=(1+\tau)t_N/2$. Then, the angular velocity over the mapped interval is fitted by the Chebyshev polynomial, given by

$$\boldsymbol{\omega}(\tau)=\sum_{i=0}^{n}\mathbf{c}_i F_i(\tau), \ n \leq N-1 \tag{11}$$

The coefficient $\mathbf{c}_i$ is determined for the case of angular velocity measurement by solving the equation as follows:

$$\begin{bmatrix} 1 & F_1(\tau_1) & \cdots & F_n(\tau_1) \\ 1 & F_1(\tau_2) & \cdots & F_n(\tau_2) \\ \vdots & \vdots & \vdots & \vdots \\ 1 & F_1(\tau_N) & \cdots & F_n(\tau_N) \end{bmatrix} \begin{bmatrix} \mathbf{c}_0^T \\ \mathbf{c}_1^T \\ \vdots \\ \mathbf{c}_n^T \end{bmatrix} = \begin{bmatrix} \boldsymbol{\omega}_1^T \\ \boldsymbol{\omega}_2^T \\ \vdots \\ \boldsymbol{\omega}_N^T \end{bmatrix} \tag{12}$$

According to the integral property of the Chebyshev polynomial [45], we have

$$G_{i,[\tau_{k-1}\ \tau_k]} \triangleq \int_{\tau_{k-1}}^{\tau_k} F_i(\tau)d\tau = \begin{cases} \left(\frac{iF_{i+1}(\tau_k)}{i^2-1}-\frac{\tau_k F_i(\tau_k)}{i-1}\right)-\left(\frac{iF_{i+1}(\tau_{k-1})}{i^2-1}-\frac{\tau_{k-1}F_i(\tau_{k-1})}{i-1}\right), & i \neq 1 \\ \frac{\tau_k^2-\tau_{k-1}^2}{2}, & i=1 \end{cases} \tag{13}$$

With the aid of (11) and (13), the angular increment is related to the fitted angular velocity by

$$\Delta\boldsymbol{\theta}_{t_k}=\int_{t_{k-1}}^{t_k}\boldsymbol{\omega}\,dt \overset{t\to\tau}{=} \frac{t_N}{2}\int_{\tau_{k-1}}^{\tau_k}\boldsymbol{\omega}\,d\tau=\frac{t_N}{2}\sum_{i=0}^{n}\mathbf{c}_i\int_{\tau_{k-1}}^{\tau_k}F_i(\tau)d\tau=\frac{t_N}{2}\sum_{i=0}^{n}\mathbf{c}_i G_{i,[\tau_{k-1}\ \tau_k]} \tag{14}$$

Then, the coefficient $\mathbf{c}_i$ in (11) is determined for the case of angular increment measurement by solving the following equation:

$$\begin{bmatrix} G_{0,[\tau_0\,\tau_1]} & G_{1,[\tau_0\,\tau_1]} & \cdots & G_{n,[\tau_0\,\tau_1]} \\ G_{0,[\tau_1\,\tau_2]} & G_{1,[\tau_1\,\tau_2]} & \cdots & G_{n,[\tau_1\,\tau_2]} \\ \vdots & \vdots & \vdots & \vdots \\ G_{0,[\tau_{N-1}\,\tau_N]} & G_{1,[\tau_{N-1}\,\tau_N]} & \cdots & G_{n,[\tau_{N-1}\,\tau_N]} \end{bmatrix} \begin{bmatrix} \mathbf{c}_0^T \\ \mathbf{c}_1^T \\ \vdots \\ \mathbf{c}_n^T \end{bmatrix} = \frac{2}{t_N} \begin{bmatrix} \Delta\boldsymbol{\theta}_1^T \\ \Delta\boldsymbol{\theta}_2^T \\ \vdots \\ \Delta\boldsymbol{\theta}_N^T \end{bmatrix} \tag{15}$$

The linear equations (7), (8), (12) and (15) could be well solved by the common least-square method.

IV. Attitude Algorithms by Taylor Series Expansion and Functional Iterative Integration

This section will apply both the Taylor series expansion and the functional iterative integration to solve the quaternion kinematic equation for attitude computation. Notably, the functional iterative integration, combined with the Chebyshev polynomial approximation, has been successfully applied for attitude computation in [39-41] and for the inertial navigation algorithm including velocity/position computation in [51]. The same approaches could be applied to other attitude parameters including the rotation vector and the Rodrigues vector without any simplification of the original differential equations, see e.g. [54].

The attitude quaternion kinematic equation is related to the angular velocity as [3, 19, 57]

$$\dot{\mathbf{q}} = \frac{1}{2}\mathbf{q} \circ \boldsymbol{\omega} \tag{16}$$

Attitude quaternion $\mathbf{q}$ is represented as a four-dimensional column vector of unit magnitude, i.e., $\mathbf{q} = \begin{bmatrix} s & \boldsymbol{\eta}^T \end{bmatrix}^T$, where s is the scalar part and $\boldsymbol{\eta}$ is the vector part. If the scalar and vector parts are regarded as a scalar quaternion and a vector quaternion, respectively, then quaternion can be alternatively written as $\mathbf{q} = s + \boldsymbol{\eta}$. The product of two quaternions is given by $\mathbf{q}_1 \circ \mathbf{q}_2 = \begin{bmatrix} s_1 & -\boldsymbol{\eta}_1^T \\ \boldsymbol{\eta}_1 & s_1\mathbf{I}_3 + \boldsymbol{\eta}_1\times \end{bmatrix} \begin{bmatrix} s_2 \\ \boldsymbol{\eta}_2 \end{bmatrix} = \begin{bmatrix} s_1 s_2 - \boldsymbol{\eta}_1^T\boldsymbol{\eta}_2 \\ s_1\boldsymbol{\eta}_2 + s_2\boldsymbol{\eta}_1 + \boldsymbol{\eta}_1\times\boldsymbol{\eta}_2 \end{bmatrix}$. Denote the Euler rotation axis and the Euler rotation angle by $\mathbf{e}$ and α respectively, the quaternion can be alternatively expressed as $\mathbf{q} = \cos\frac{\alpha}{2} + \mathbf{e}\sin\frac{\alpha}{2}$. $\boldsymbol{\omega}$ is the angular velocity vector quaternion with zero scalar part, formed by the three-dimensional angular velocity vector.

A. QuatTaylor by Taylor Series Expansion

The j-th order derivative of the quaternion can be recursively computed as

$$\mathbf{q}^{(j)}(0) = \frac{1}{2}\left(\mathbf{q}\circ\boldsymbol{\omega}\right)^{(j-1)}\Big|_{t=0} = \frac{1}{2}\sum_{i=0}^{j-1}\binom{j-1}{i}\mathbf{q}^{(j-1-i)}(0)\circ\boldsymbol{\omega}^{(i)}(0) \tag{17}$$

Explicitly, $\mathbf{q}^{(0)}(0) = \mathbf{q}(0)$, $\mathbf{q}^{(1)}(0) = \frac{1}{2}\mathbf{q}(0)\circ\mathbf{d}_0$ and $\mathbf{q}^{(2)}(0) = \frac{1}{2}\left(\mathbf{q}^{(1)}(0)\circ\mathbf{d}_0 + \mathbf{q}^{(0)}(0)\circ\mathbf{d}_1\right)$, etc.

Then, the Taylor series approximation (3) can be explicitly written as

$$\mathbf{q}(t)=\frac{1}{2}\sum_{j=0}^{m}\left(\sum_{i=0}^{j-1}\binom{j-1}{i}\mathbf{q}^{(j-1-i)}(0)\circ\boldsymbol{\omega}^{(i)}(0)\right)\frac{t^j}{j!} \tag{18}$$

It should be noted that the Taylor series approximation in (18) is a time polynomial that actually reconstructs the whole attitude history over the time interval $[t_0 \;\; t_N]$ in which the N gyroscope samples are measured, sharing the same advantage of the attitude algorithms by functional iterative integration [16, 43, 44].

B. QuatFIter-np by Functional Iterative Integration (Normal Polynomial) [3]

With the angular velocity polynomial in (6), the functional iterative integration (4) is applied to the attitude quaternion rate equation (16), yielding

$$\mathbf{q}_j(t)=\mathbf{q}(0)+\frac{1}{2}\int_0^t\mathbf{q}_{j-1}\circ\boldsymbol{\omega}\,dt=\mathbf{q}(0)+\frac{1}{2}\int_0^t\mathbf{q}_{j-1}(t)\circ\sum_{i=0}^{n}\mathbf{d}_i t^i\,dt,\quad j=1,2,\ldots \tag{19}$$

Suppose the attitude quaternion at the (j-1)-th iteration is represented by a normal polynomial of order m_{j-1}, i.e., $\mathbf{q}_{j-1}(t)=\sum_{k=0}^{m_{j-1}}\mathbf{b}_{j-1,k}t^k$. Substituting into (19) gives

$$\begin{aligned}\mathbf{q}_j(t)&=\mathbf{q}(0)+\frac{1}{2}\int_0^t\sum_{k=0}^{m_{j-1}}\mathbf{b}_{j-1,k}t^k\circ\sum_{i=0}^{n}\mathbf{d}_i t^i\,dt\\&=\mathbf{q}(0)+\frac{1}{2}\sum_{k=0}^{m_{j-1}}\sum_{i=0}^{n}\frac{\mathbf{b}_{j-1,k}\circ\mathbf{d}_i}{k+i+1}t^{k+i+1},\quad j=1,2,\ldots\end{aligned} \tag{20}$$

It can be seen that the polynomial order of attitude quaternion grows quickly by $m_j=m_{j-1}+n+1$. In the explicit form, $\mathbf{q}_0(t)=\mathbf{q}(0)$ and $\mathbf{q}_1(t)=\mathbf{q}(0)+\frac{1}{2}\mathbf{q}(0)\circ\sum_{i=0}^{n}\frac{\mathbf{d}_i}{i+1}t^{i+1}$, etc.

Note that Eq. (20) could be iterated by updating the normal polynomial coefficients only and truncating the normal polynomials at each iteration to avoid fast order growing, as done in [41]. The polynomial truncation order, denoted by m_T hereafter, also acts as the highest order of derivative to those algorithms by the Taylor series expansion. The iteration times could be controlled by some pre-defined maximum or stopping criterion given in the sequel.

C. QuatFIter by Functional Iterative Integration (Chebyshev Polynomial)

With the angular velocity polynomial given by (11), the functional iterative integration approach (4) is applied to solve the quaternion rate equation [41]

$$\mathbf{q}_j=\mathbf{q}(0)+\frac{1}{2}\int_0^t\mathbf{q}_{j-1}\circ\boldsymbol{\omega}\,dt=\mathbf{q}(0)+\frac{t_N}{4}\int_{-1}^{\tau}\mathbf{q}_{j-1}\circ\boldsymbol{\omega}\,d\tau \tag{21}$$

Assume $\boldsymbol{\omega}$ and the quaternion estimate at the (j-1)-th iteration is given by a weighted sum of Chebyshev polynomials, say $\mathbf{q}_{j-1}\triangleq\sum_{k=0}^{m_{j-1}}\mathbf{b}_{j-1,k}F_k(\tau)$ where m_{j-1} is the maximum

[3] Abbreviation 'FIter' stands for Functional Iterative integration; 'np' stands for normal polynomial.

degree and $\mathbf{b}_{j-1,k}$ is the coefficient of the k^{th}-degree Chebyshev polynomial at the (j-1)-th iteration. Substituting it, together with (10) and (11), into (21)

$$\mathbf{q}_j(\tau) = \mathbf{q}(0) + \frac{t_N}{8}\sum_{k=0}^{m_{j-1}}\sum_{i=0}^{n}\mathbf{b}_{j-1,k}\circ\mathbf{c}_i\left(G_{k+i,[-1\ \tau]} + G_{|k-i|,[-1\ \tau]}\right) \tag{22}$$

where $G_{i,[-1\ \tau]}$ is the integrated i^{th}-degree Chebyshev polynomial over the interval $[-1\ \tau]$, as defined in (13).

Similarly, Eq. (22) could be iterated by updating the Chebyshev polynomial coefficients only and making necessary polynomial truncation at each iteration to avoid fast order growing [39-41].

V. Numerical Results and Algorithm Comparison

Simulations are performed in this section under the classical coning motion scenario to evaluate these algorithms. The coning motion has explicit analytical expressions in the angular velocity and the attitude parameter, so it has been widely accepted as a standard criterion for algorithm accuracy assessment in the inertial navigation field [3, 7]. It is not uncommon in practice with a large excitation of attitude drift error, e.g., in situations of angular vibration or complex rotation. The angular velocity of the classical coning motion is described by $\boldsymbol{\omega} = \Omega\left[-2\sin^2(\alpha/2)\ \ -\sin(\alpha)\sin(\Omega t)\ \ \sin(\alpha)\cos(\Omega t)\right]^T$, with the true rotation vector $\boldsymbol{\sigma} = \alpha\left[0\ \ \cos(\Omega t)\ \ \sin(\Omega t)\right]^T$ and the true quaternion $\mathbf{q} = \cos(\alpha/2) + \sin(\alpha/2)\left[0\ \ \cos(\Omega t)\ \ \sin(\Omega t)\right]^T$. In the above, α denotes the coning angle and $\Omega = 2\pi f_c$ denotes the angular frequency of the coning motion (unit: rad/s) and f_c is the coning frequency (unit: Hz). The angular increment measurement is assumed and the sampling rate is nominally set to $f_s = 1000$ Hz.

The following principal angle metric is used to quantify the attitude computation error

$$\varepsilon_{att} = 2\left|\left[\mathbf{q}^*\circ\hat{\mathbf{q}}\right]_{2:4}\right| \tag{23}$$

where $\hat{\mathbf{q}}$ denotes the quaternion estimate computed by attitude algorithms, and the operator $[\cdot]_{2:4}$ takes the vector part of the error quaternion. Note that the single-axis drift error metric widely used in most mainstream algorithms does not account for errors in the other two axes, perhaps misleading in motions with large coning angles [58]. If the used attitude parameter is other than quaternion, then the computed result needs to be transformed to the corresponding quaternion for error quantification, as done in [54]. The polynomial order of the fitted angular velocity (6) is uniformly set to $n = N-1$, if not explicitly stated.

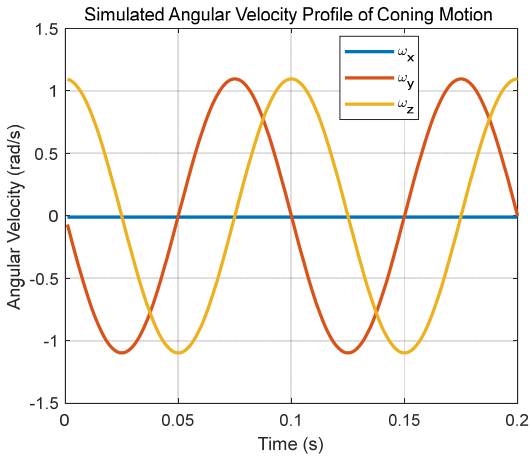

Fig. 1 Angular velocity profile of classical coning motion.

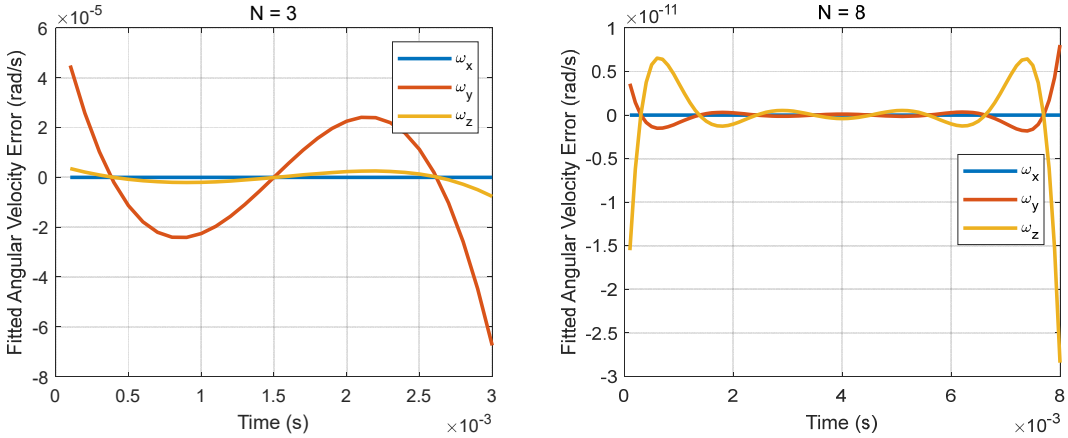

Fig. 2 Errors of fitted angular velocity for $N = 3$ and 8.

A. Fitted Angular Velocity Polynomial and Reconstructed Attitude

Figure 1 plots the angular velocity profile of the classical coning motion, where the coning angle is set to $\alpha = 1$ degree with the coning frequency $f_c = 10$ Hz. Figure 2 presents the errors of the fitted angular velocity by the normal polynomial (6) or by the Chebyshev polynomial (11) during the first update interval, for the number of samples $N = 3$ and 8. It shows that using more samples leads to much more accurate fitted angular velocity, making it possible to acquire more accurate attitude. Note that an erroneous angular velocity cannot in general be compensated in the subsequent attitude computation process. The work of RodFIter in [39] has thrown lights on this fact in the case of the Rodrigues vector (Theorem 2 therein). The two kinds of polynomials have identical angular velocity fitting errors but their coefficients differ much (cf. Fig. 4 in the sequel).

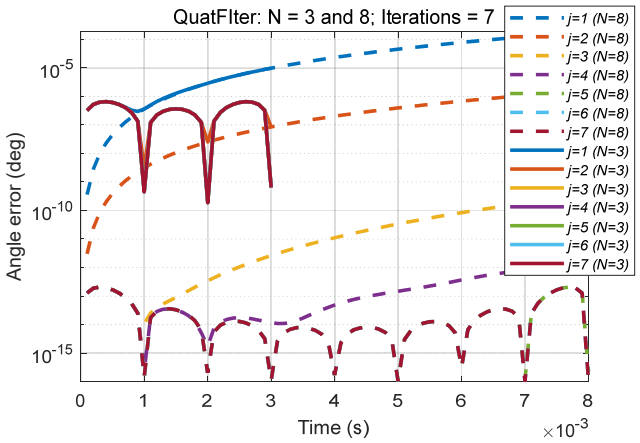

Fig. 3 Attitude errors of QuatFIter across seven iterations for $N = 3$ (sold lines) and 8 (dashed lines).

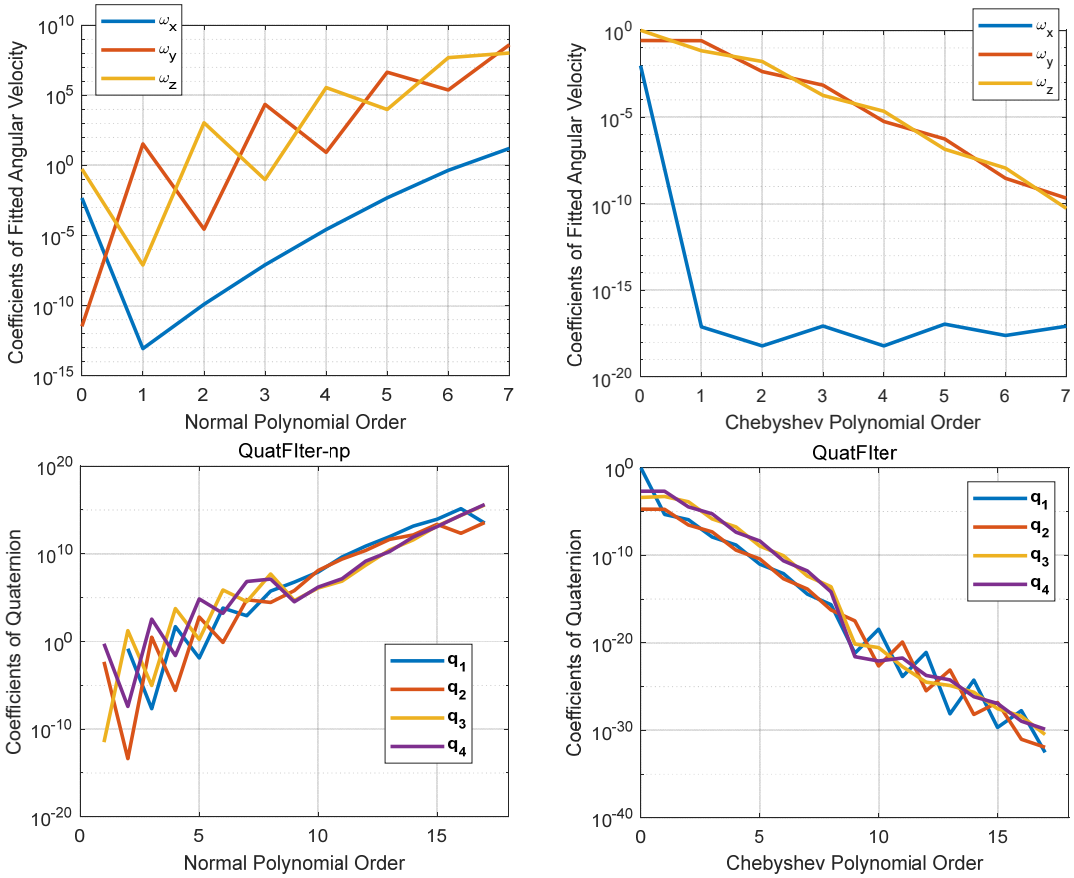

Fig. 4 Polynomial coefficients of fitted angular velocity and computed quaternion by QuatFIter-np (left) and QuatFIter (right) for $N = 8$.

Taking the QuatFIter algorithm as a demonstration (polynomial truncation order set to

$m_T = N + 9$), Figure 3 plots the principal angle errors of the reconstructed attitudes over the first iteration interval, across seven iterations for the cases of $N = 3$ and 8. The angle error reduces and converges as the iteration goes on. Because the fitted angular velocity has much better accuracy, the attitude error with $N = 8$ is significantly smaller. Additionally, regarding the converged results (after two iterations with $N = 3$; after four iterations with $N = 8$), the attitude errors turn to have sharp drops at the sampling instants. This apparent 'n-shape' phenomenon is an indication of insufficient fitting of the angular velocity polynomials by the current number of gyroscope samples. Figure 4 presents the polynomial coefficients of the fitted angular velocities for the case of $N = 8$, as well as those of the computed quaternions at the 7th iteration by QuatFIter-np and QuatFIter. Along with the increasing order, the magnitude of the normal polynomial quickly increases while that of the Chebyshev polynomial swiftly decreases. The trend is observed in both the fitted angular velocities and the computed quaternions.

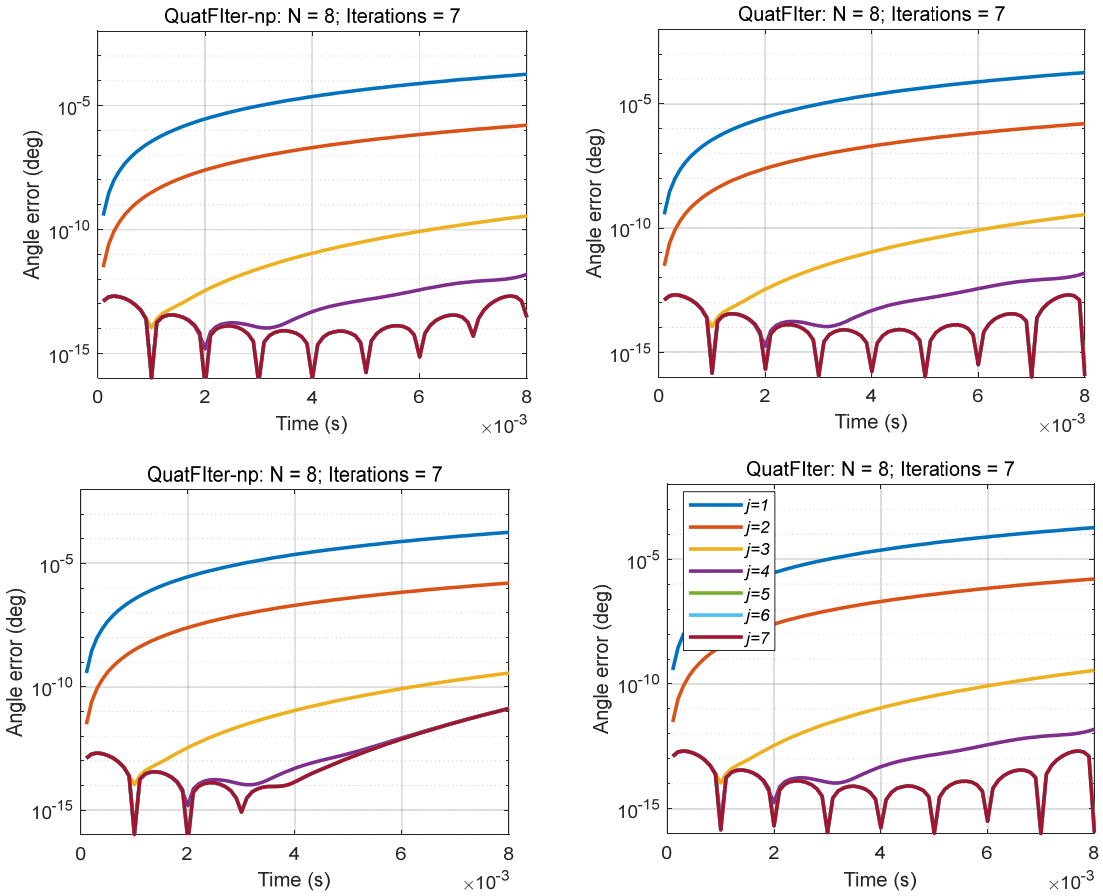

Fig. 5 Truncation effect on QuatFIter-np and QuatFIter (Top: $m_T = N + 5$; bottom: $m_T = N + 2$).

B. Polynomial Truncation and Iteration Times

Figure 5 examines the effect of two polynomial truncation orders ($m_T = N+5, N+2$) on QuatFIter-np and QuatFIter across seven iterations. We see that the QuatFIter-np is more vulnerable to polynomial truncation, indicating that the normal polynomial has inferior functional representation capability than the Chebyshev polynomial does. In other words, the Chebyshev polynomial requires relatively fewer terms to achieve the same accuracy, an excellent property favorable to numerical computation [45].

Figure 6 compares the attitude errors and quaternion-norm errors of QuatFIter-np and QuatTaylor, across fifteen iterations for the case of $N = 8$. The polynomial truncation order is still set to $m_T = N+9$ for both algorithms. We see that it takes more iterations for QuatTaylor to reach comparable accuracy, e.g., fourteen iterations to reach the convergence in contrast to only five iterations for QuatFIter-np. This is owed to the fast increase of normal polynomial orders in QuatFIter-np, as shown in (20), while the normal polynomial

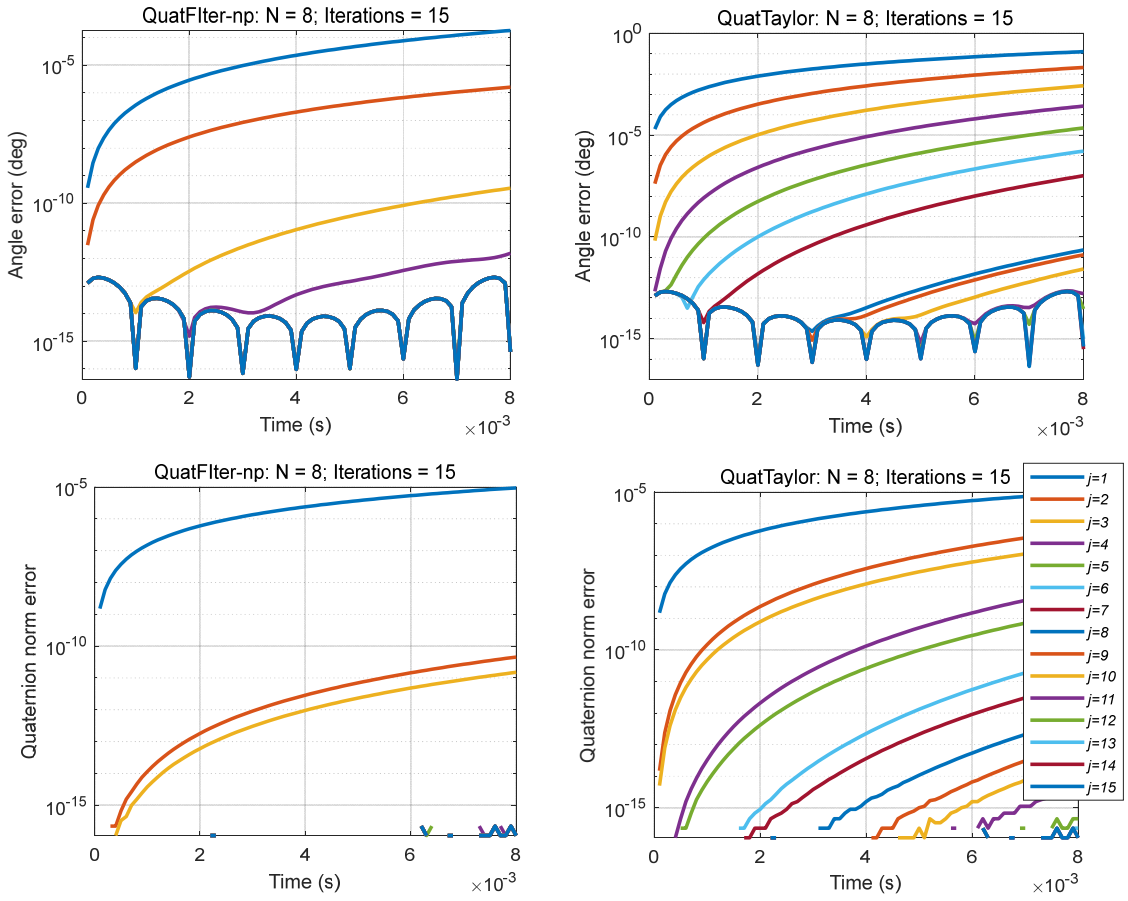

Fig. 6 Attitude errors and quaternion-norm errors of QuatFIter-np and QuatTaylor. Note the order of legend colors used to denote different iterations are the same throughout the paper.

order of QuatTaylor increases one by one along with each iteration. From the quaternion kinematic equation (16), it can be readily shown that the norm of quaternion is naturally preserved, i.e., $d\left(\mathbf{q}^T\mathbf{q}\right)/dt = 2\mathbf{q}^T\dot{\mathbf{q}} = \mathbf{q}^T\left(\mathbf{q}\circ\boldsymbol{\omega}\right) = \begin{bmatrix}1 & \mathbf{0}_{3\times1}\end{bmatrix}\boldsymbol{\omega} = 0$, if only we could compute the kinematic equation accurately, whether by Taylor expansion or iterative integration. We see in Fig. 6 that the quaternion norm gradually approaches to unity because the initial quaternion is of unit norm, which sets the foundation for QuatFIter [41] that used quaternion directly for attitude computation.

It should be highlighted that the above conclusions derived from Figs. 5-6 are independent of the specific attitude parameters [54], which is in favor of the functional iterative integration combined with the Chebyshev polynomial for attitude computation. For a stopping criterion of iteration, the algorithm by Taylor series expansion could check if the highest-order term (HOT) is negligible relative to the require attitude accuracy, and those algorithms by functional iterative integration could use the discrepancy of polynomial coefficients (DPC) between successive iterations, namely, $\sqrt{\sum_{k=0}^{m_T}\left|\mathbf{b}_{j+1,k}-\mathbf{b}_{j,k}\right|^2}$.

C. Accuracy Comparison

A comprehensive accuracy comparison is performed next for the case of $N = 8$, with the coning frequency ranging 1-200 Hz. The HOT and DPC iteration-stopping criteria are respectively used in the Taylor expansion-derived algorithm and the functional iterative integration-derived algorithms. Figure 7 presents the attitude errors accumulated over one second as a function of relative frequency f_c/f_s (the analogy of the attitude error drift [29]) for QuatTaylor and QuatFIter, against the mainstream 2/3-sample algorithms[4] [10]. The results of QuatFIter-np is omitted because it is found to be nearly identical to those of

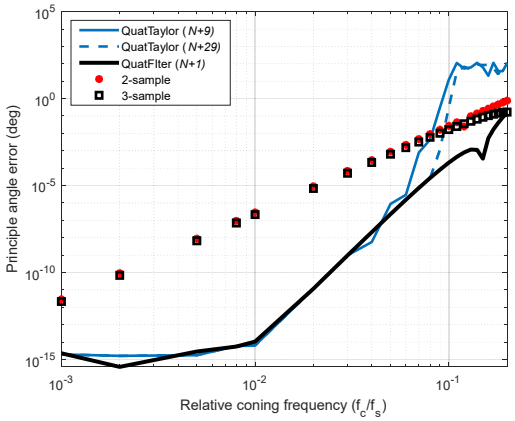

Fig. 7 Attitude errors as function of relative frequency for $N = 8$, as compared with the mainstream 2/3-sample algorithms.

[4] The unoptimized 3-sample algorithm is used, as given in (7) therein, as the current paper reasonablly assumes no priori knowldege of the experienced attitude motion. The optimized version instead would not affect the main conclusion.

QuatTaylor. We see that all algorithms have comparable accuracy while the coning frequency stays below 60 Hz, linearly increasing with respect to the relative frequency. Specifically, they all reach the machine precision for coning frequency less than 10 Hz. If the coning frequency goes up further, however, QuatTaylor, with the truncation order $m_T = N + 9$, begins to deteriorate and become even worse than the mainstream 2/3-sample algorithms for over 70 Hz. When the truncation order is set to $m_T = N + 29$, its accuracy does not decline until the coning frequency is larger than 80 Hz. In contrast, with a constant truncation order $m_T = N + 1$, the accuracy of QuatFIter is uniformly the best over the whole frequency range, approaching those of the mainstream algorithms at the right end. It is observed in our simulations that higher truncation order would not bring further accuracy improvement to the QuatFIter. This significant advantage is largely owed to the excellent functional representation capability and numerical stability of the Chebyshev polynomial. The effect of different gyroscope samples on the accuracy is further examined at the coning frequency of 100 Hz and 200 Hz in Fig. 8. It appears that QuatFIter and QuatTaylor has comparable accuracy at small *N*. The underlying reason is that the polynomial order is too low to sufficiently represent the angular velocity and the approximation error dominates the attitude error. Along with the increased number of gyroscope samples, the attitude error of QuatFIter generally reduces and in contrast QuatTaylor begins to rise when the number of gyroscope samples is greater than 5 (for 100 Hz) or 3 (for 200 Hz).

The error rising of QuatTaylor appears odd, so the case of $f_c = 100$ Hz is particularly examined. Figure 9 presents attitude errors for two update intervals using the polynomial truncation orders $m_T = N + 29$ and $m_T = N + 49$. With the truncation order increased, QuatTaylor improves in accuracy as expected. However, contrary to the prediction that their accuracies could be unlimitedly improved by further increasing the truncation order, we have observed that QuatTaylor encounters numerical failures when the truncation order is larger than 150. Of special interest is the 'u-shape' profile in the QuatFIter that has oscillated peaks close to both ends of iteration intervals. It is the famous Runge's phenomenon [59] that is ubiquitous in high-order polynomial interpolation for equispaced

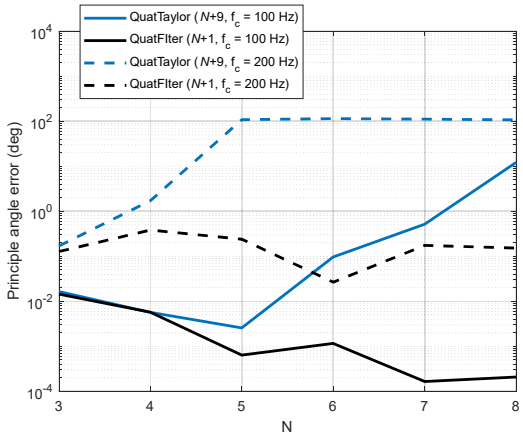

Fig. 8 Attitude errors across different *N*s for coning frequency of 100 Hz and 200 Hz.

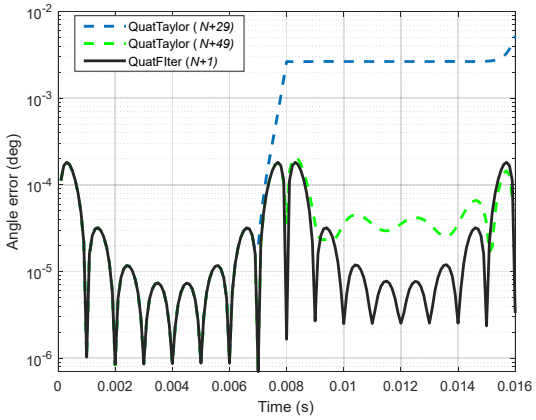

Fig. 9 Attitude errors in two update intervals at coning frequency of 100 Hz for $N = 8$, with truncation order $m_T = N + 29$ and $N + 49$.

samples, which can also be apparently identified in Fig. 2 for the fitted angular velocity with $N = 8$. An interesting thing is observed in the case of $N = 5$ samples, as shown in Fig. 10 in which the algorithm results overlap (with the results of Fig. 9 as the background). In specific, QuatTaylor demonstrates better accuracy than it does in Fig. 9 ($N = 8$). This unusual observation is believed to be incurred by the Runge's phenomenon in equispaced sampling, so is the numerical failure encountered above. Supposedly, the technique of depressing the Runge's phenomenon (e.g. using multiple integrals of gyroscope measurements [31, 53]) could be used to improve the derived algorithms including the already well-performing QuatFIter.

Finally, a practical situation with noisy gyroscope measurement is investigated, as the high-order/sample algorithms tend to be much more sensitive to narrow-band noises that might lead to pseudo-coning [31]. Noise errors with an angle random walk of 0.001

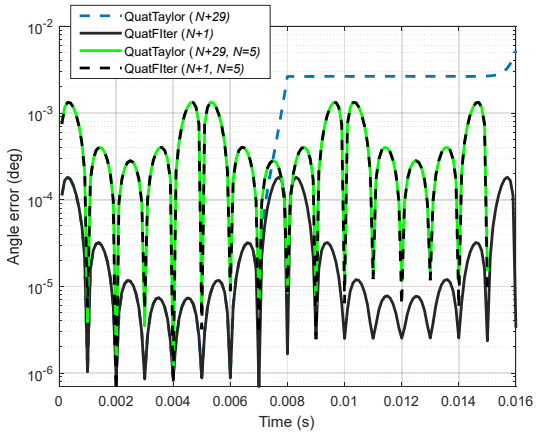

Fig. 10 Attitude errors in three update intervals for $N = 5$ samples at coning frequency of 100 Hz, as compared with the result for $N = 8$ in Fig. 9.

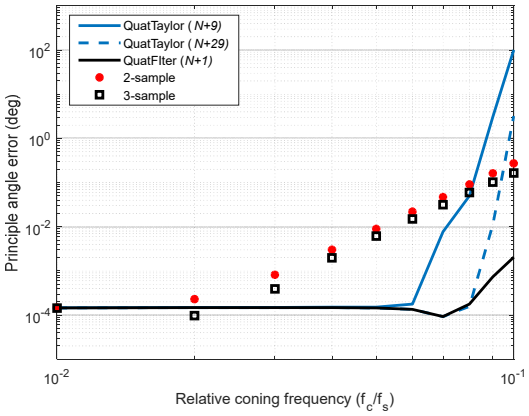

Fig. 11 Attitude errors as function of relative frequency ($N = 8$) for navigation-grade gyroscope measurements.

$\deg/\sqrt{h}$, comparable to a navigation-grade inertial navigation system, are considered. A common set of random gyroscope noises are generated and fed to all algorithms for uniform comparison. Figure 11 plots the attitude errors in ten seconds as the function of relative frequency for $N = 8$. For coning frequencies below 20 Hz, all derived algorithms have similar accuracy with the mainstream 2/3-sample algorithms, as the noise dominates the attitude accuracy (cf. Fig. 7). The derived algorithms are comparable to each other when the coning frequency is below about 60-80 Hz. The performance ranking keeps the same with the noise-free case in Fig. 7.

In closing, the accuracy of the considered algorithms is governed by angular velocity approximation quality and the differential equation solution of Taylor series expansion or functional iterative integration [39-41]. The latter can in principle achieve machine precision by iteratively solving the exact form of attitude differential equation, surmounting the fundamental limitation of mainstream algorithms using simplified rate equations. The angular velocity approximation quality, however, depends on the smoothness of the inertial inputs, noises and the number of gyroscope samples. Generally, more gyroscope samples are used, better angular velocity approximation accuracy would be obtained. But there is a theoretical boundary set by Runge phenomenon, although polynomials in theory are able to approximate any smooth function as well as possible. Hopefully, techniques depressing the Runge's phenomenon could be exploited to further improve the accuracy of the derived algorithms.

The algorithm application of QuatFIter (embedded in iNavFIter [51]) are available online at https://www.researchgate.net/project/Motion-Representation-and-Computation-Inertial-Navigation-and-Beyond (project log). Interested readers are welcome to assess the algorithms.

VI. Conclusions

This paper poses the strapdown attitude computation as seeking the general solutions to the kinematic equations of attitude parameters. Two basic approaches are briefly reviewed, namely, the Taylor series expansion approach which was developed in the iterative form to account for the high-order angular rate derivatives and the Picard-type technique which was recently developed by the first author in the form of functional iterative integration approach. Then, three attitude algorithms have been derived by the two basic approaches, based on the attitude parameter of quaternion. Numerical tests under classical coning motions are carried out to compare the algorithms, refining the conclusions drawn in previous papers on the functional iterative integration approach. It is observed that in the relative frequency range when the coning to sampling frequency ratio is below 0.06-0.2 (depending on the number of gyroscope samples and the chosen polynomial truncation order), three algorithms have the same order of accuracy if the same number of samples are used to fit the angular velocity over the iteration interval; in the range of higher relative frequency, QuatFIter performs better in both accuracy and robustness to the Runge phenomenon than the other two algorithms do for a larger number of gyroscope samples, thanks to the unique properties of Chebyshev polynomial. Notably, QuatFIter allows a lower truncation order, while the other two algorithms require significantly higher truncation order and might even encounter numerical failure.

Funding Sources

The first author of the paper was supported in part by National Key R&D Program of China (2018YFB1305103) and National Natural Science Foundation of China (61673263).

References

[1] F. L. Markley, J. L. Crassidis, *Fundamentals of Spacecraft Attitude Determination and Control*: Springer, 2014.

[2] D. H. Titterton, J. L. Weston, *Strapdown Inertial Navigation Technology*, 2nd ed.: the Institute of Electrical Engineers, London, United Kingdom, 2007.

[3] P. D. Groves, *Principles of GNSS, Inertial, and Multisensor Integrated Navigation Systems*, 2nd ed.: Artech House, Boston and London, 2013.

[4] D. A. Tazartes, "Inertial Navigation: From Gimbaled Platforms to Strapdown Sensors," *IEEE Trans. on Aerospace and Electronic Systems,* vol. 47, pp. 2292-2299, 2010.

[5] J. G. Mark, D. A. Tazartes, "Tuning of Coning Algorithms to Gyro Data Frequency Response Characteristics," Journal of Guidance, Control, and Dynamics," vol. 24, pp. 641-647, 2001.

[6] P. G. Savage, "A new second-order solution for strapped-down attitude computation," in *AIAA/JACC Guidance and Control Conference*, 1966.

[7] "A study of the critical computational problems associated with strapdown inertial navigation systems," NASA CR-968 by United Aircraft Corporation, 1968.

[8] J. W. Jordan, "An accurate strapdown direction cosine algorithm," NASA TN-D-5384, 1969.

[9] J. E. Bortz, "A new mathematical formulation for strapdown inertial navigation," *IEEE Trans. on Aerospace and Electronic Systems,* vol. 7, pp. 61-66, 1971.

[10] R. Miller, "A new strapdown attitude algorithm," *Journal of Guidance, Control, and Dynamics,* vol. 6, pp. 287-291, 1983.

[11] M. B. Ignagni, "Optimal strapdown attitude integration algorithms," *Journal of Guidance, Control, and*

Dynamics, vol. 13, pp. 363-369, 1990.
[12] M. B. Ignagni, "Efficient class of optimized coning compensation algorithm," *Journal of Guidance, Control, and Dynamics,* vol. 19, pp. 424-429, 1996.
[13] P. G. Savage, "Strapdown inertial navigation integration algorithm design, part 1: attitude algorithms," *Journal of Guidance, Control, and Dynamics,* vol. 21, pp. 19-28, 1998.
[14] Y. A. Litmanovich, V. M. Lesyuchevsky, V. Z. Gusinsky, "Two new classes of strapdown navigation algorithms," *Journal of Guidance, Control, and Dynamics,* vol. 23, pp. 34-44, 28-30, Jun. 2000.
[15] P. Savage, "Down-Summing Rotation Vectors For Strapdown Attitude Updating (SAI WBN-14019)," Strapdown Associates (http://strapdownassociates.com/Rotation%20Vector%20Down_Summing.pdf) 2017.
[16] Y. A. Litmanovich, J. G. Mark, "Progress in Strapdown Algorithm Design at the West and East as Appeared at Saint Petersburg Conferences: Decade Overview," in *Saint-Petersburg International Conference on Integrated Navigational Systems*, Russia, 2003.
[17] J. G. Lee, Y. J. Yoon, J. G. Mark, D. A. Tazartes, "Extension of strapdown attitude algorithm for high-frequency base motion," *Journal of Guidance, Control, and Dynamics,* vol. 13, pp. 738-743, 1990.
[18] Z. Xu, J. Xie, Z. Zhou, J. Zhao, Z. Xu, "Accurate Direct Strapdown Direction Cosine Algorithm," *IEEE Trans. on Aerospace and Electronic Systems,* vol. 55, pp. 2045-2053, 2019.
[19] V. N. Branets, I. P. Shmyglevsky, *Application of Quaternions to the Problems of Rigid Body Orientation*: Nauka (in Russian), 1973.
[20] A. P. Panov, *Mathematical Fundamentals of Inertial Navigation Theory*: Kiev, Naukova Dumka (in Russian), 1994.
[21] C. Rucker, "Integrating Rotations Using Nonunit Quaternions," *IEEE Robotics and Automation Letters,* vol. 3, pp. 2779-2986, 2018.
[22] J. Park, W.-K. Chung, "Geometric integration on euclidean group with application to articulated multibody systems," *IEEE Trans. on Robotics,* vol. 21, pp. 850-863, 2005.
[23] M. S. Andrle, J. L. Crassidis, "Geometric Integration of Quaternions," *Journal of Guidance, Control, and Dynamics,* vol. 36, pp. 1762-1767, 2013.
[24] M. Boyle, "The Integration of Angular Velocity," *Advances in Applied Clifford Algebras,* vol. 27, pp. 2345–2374, 2017.
[25] P. Krysl, L. Endres, "Explicit Newmark/Verlet algorithm for time integration of the rotational dynamics of rigid bodies," *International Journal for Numerical Methods in Engineering,* vol. 62, pp. 2154–2177, 2005.
[26] E. Hairer, C. Lubich, G. Wanner, *Geometric Numerical Integration: Structure Preserving Algorithms for Ordinary Differential Equations*. New York, NY, USA: Springer-Verlag, 2006.
[27] H. Musoff, J. H. Murphy, "Study of strapdown navigation attitude algorithm," *Journal of Guidance, Control, and Dynamics,* vol. 18, pp. 287-290, 1995.
[28] V. Z. Gusinsky, V. M. Lesyuchevsky, Y. A. Litmanovich, H. Musoff, G. T. Schmidt, "Optimization of a strapdown attitude algorithm for a stochastic motion," *Navigation: Journal of The Institute of Navigation,* vol. 44, pp. 163-170, 1997.
[29] V. Z. Gusinsky, V. M. Lesyuchevsky, Y. A. Litmanovich, H. Musoff, G. T. Schmidt, "New procedure for deriving optimized strapdown attitude algorithm," *Journal of Guidance, Control, and Dynamics,* vol. 20, pp. 673-680, 1997.
[30] D. A. Tazartes, J. G. Mark, "Coning compensation in strapdown inertial navigation systems," US Patent US005828980A, 1997.
[31] Y. A. Litmanovich, "Use of angular rate multiple integrals as input signals for strapdown attitude algorithms," in *Symposium Gyro Technology*, Stuttgart, Germany, 1997.
[32] V. M. Slyusar, "Current Issues of Designing SINS Attitude Algorithms. Part 3. Algorithms Analysis and Synthesiswith Account for Gyros Frequency Response Effect," *Gyroscopy and Navigation (in Russian),* vol. 4, pp. 21-36, 2006.
[33] P. Savage, "Modern Strapdown Attitude Algorithms And Their Accuracy, Versus Accuracy Requirements For Unaided Strapdown Inertial Navigation (SAI WBN-14025)," Strapdown Associates (http://strapdownassociates.com/Algorithm%20Accuracy%20Vs%20%20INS%20Requirements.pdf) 2020.
[34] C. I. Sukenik, "Application of ultracold molecules to inertial sensing for navigation," ADA146124, 2004.
[35] M. Kasevich. (2002). *Science and technology prospects for ultra-cold atoms*. Available: www7.nationalacademies.org/bpa/kasevich_CAMOS_021124.pdf

[36] M. Ignagni, "Enhanced Strapdown Attitude Computation," *Journal of Guidance Control and Dynamics,* vol. 43, pp. 1220–1224, 2020.
[37] M. Wang, W. Wu, J. Wang, X. Pan, "High-order attitude compensation in coning and rotation coexisting environment," *IEEE Trans. on Aerospace and Electronic Systems,* vol. 51, pp. 1178-1190, 2015.
[38] M. Wang, W. Wu, X. He, G. Yang, H. Yu, "Higher-order Rotation Vector Attitude Updating Algorithm," *Journal of Navigation,* vol. 72, pp. 721-740, 2019.
[39] Y. Wu, "RodFIter: Attitude Reconstruction from Inertial Measurement by Functional Iteration," *IEEE Trans. on Aerospace and Electronic Systems,* vol. 54, pp. 2131-2142, 2018.
[40] Y. Wu, Q. Cai, T.-K. Truong, "Fast RodFIter for Attitude Reconstruction from Inertial Measurement," *IEEE Trans. on Aerospace and Electronic Systems,* vol. 55, pp. 419-428, 2019.
[41] Y. Wu, G. Yan, "Attitude Reconstruction from Inertial Measurements: QuatFIter and Its Comparison with RodFIter," *IEEE Trans. on Aerospace and Electronic Systems,* vol. 55, pp. 3629-3639, 2019.
[42] G. Yan, J. Weng, X. Yang, Y. Qin, "An Accurate Numerical Solution for Strapdown Attitude Algorithm based on Picard iteration," *Journal of Astronautics,* vol. 38, pp. 65-71, 2017.
[43] K. E. Atkinson, W. Han, D. E. Stewart, *Numerical Solution of Ordinary Differential Equations*: John Wiley and Sons, 2009.
[44] R. E. Moore, *Methods and Applications in interval analysis*. Philadelphia: SIAM, 1979.
[45] W. H. Press, *Numerical Recipes: the Art of Scientific Computing*, 3rd ed. Cambridge; New York: Cambridge University Press, 2007.
[46] M. B. Ignagni, "On the orientation vector differential equation in strapdown inertial systems," *IEEE Trans. on Aerospace and Electronic Systems,* vol. 30, pp. 1076-1081, 1994.
[47] V. M. Slyusar, "Current Issues of Designing SINS Attitude Algorithms. Part 1. Amplitude Extension of the Algorithms Application Field," *Gyroscopy and Navigation (in Russian),* vol. 2, pp. 61-74, 2006.
[48] Y. Wu, "Rigid Motion Reconstruction by Functional Iteration," in *Inertial Sensors and Systems - Symposium Gyro Technology (ISS-SGT)*, Karlsruhe, Germany, 2017.
[49] Y. Wu, "Fast RodFIter for Precision Attitude Computation," in *Inertial Sensors and Systems - Symposium Gyro Technology (ISS-SGT)*, Braunschweig, Germany, 2018.
[50] Y. Wu, "Next-Generation Inertial Navigation Computation Based on Functional Iteration," in *International Conference on Integrated Navigation Systems (ICINS) & Inertial Sensors and Systems - Symposium Gyro Technology (ISS-SGT)*, Saint Petersburg, Russia; Braunschweig, Germany, 2019.
[51] Y. Wu, "iNavFIter: Next-Generation Inertial Navigation Computation Based on Functional Iteration," *IEEE Trans. on Aerospace and Electronic Systems,* vol. 56, pp. 2061-2082, 2020.
[52] C. W. Clenshaw, H. J. Norton, "The Solution of Nonlinear Ordinary Differential Equations in Chebyshev Series," *Computer Journal,* vol. 6, pp. 88-92, 1963.
[53] Y. A. Litmanovich, V. M. Lesyuchevsky, V. Z. Gusinsky, "Strapdown attitude/navigation algorithms with angular rate/specific force multiple integrals as input signals," in *ION 55th Annual Meeting*, Cambridge, MA, 1999.
[54] Y. Wu, Y. A. Litmanovich, "Strapdown Attitude Computation: Functional Iterative Integration versus Taylor Series Expansion," https://arxiv.org/abs/1909.09935, 2019.
[55] E. Hairer, S. P. Nørsett, G. Wanner, *Solving Ordinary Differential Equations I*. Berlin Heidelberg: Springer-Verlag, 2008.
[56] W. J. Rugh, *Linear System Theory*, 2nd ed. New Jersey: Prentice-Hall, 1996.
[57] V. N. Branets, I. P. Shmyglevsky, *Introduction to the Theory of Strapdown Inertial Navigation System*: Moscow, Nauka (in Russian), 1992.
[58] R. Peng, G. Yan, Y. Qin, "Limitations of residual error estimate for classic coning compensation algorithm," presented at the The Ninth International Conference on Electronic Measurement & Instruments, 2009.
[59] L. N. Trefethen, *Approximation Theory and Approximation Practice*: SIAM, 2012.